ELSEVIER

Biochemical Pharmacology 63 (2002) 1831–1842

Biochemical Pharmacology

# Involvement of microtubules and mitochondria in the antagonism of arsenic trioxide on paclitaxel-induced apoptosis

Manon Carré[a], Gérard Carles[a], Nicolas André[a], Soazig Douillard[a], Joseph Ciccolini[b], Claudette Briand[a], Diane Braguer[a,*]

[a]*UMR CNRS 6032, Faculty of Pharmacy, University of La Méditerranée, 27 Bd Jean Moulin, 13005 Marseille, France*
[b]*UPRES-EA CNRS 3286, Faculty of Pharmacy, University of La Méditerranée, 27 Bd Jean Moulin, 13005 Marseille, France*

Received 2 November 2001; accepted 26 February 2002

**Abstract**

Arsenic trioxide ($As_2O_3$) at low concentrations (1–10 μM) is effective in the treatment of acute promyelocytic leukemia (APL) and lymphoma and is in clinical trials for treatment of solid tumors. Paclitaxel, an antimicrotubule agent, is highly efficacious in the treatment of adult tumors and is in clinical evaluation in childhood tumors. This study is the first to investigate the combination of arsenic and paclitaxel in the range of clinically achievable concentrations. We found that the simultaneous combination was antagonistic on proliferation of the neuroblastoma SK-N-SH cell line by using the combination index (CI) method. Moreover, a $40 \pm 5\%$ decrease in paclitaxel-induced apoptosis in cells co-treated with $As_2O_3$ confirmed the antagonism. The mechanism of antagonism was studied at the cellular level with 200 nM paclitaxel, twice the $IC_{50}$ value, and with 1 μM $As_2O_3$ which administered singly did not affect cell survival or the microtubule network. $As_2O_3$ antagonized the effects of paclitaxel on tubulin and microtubules. Paclitaxel-induced mitotic block was decreased by $20 \pm 2\%$ and bundles induced by 200 nM paclitaxel were less condensed in the presence of 1 μM $As_2O_3$. $As_2O_3$ (10–200 μM) induced a concentration-dependent inhibition of tubulin polymerization *in vitro* which was maintained in presence of paclitaxel. Spectrophotometric and spectrofluorometric measurements indicated an interaction of $As_2O_3$ with tubulin SH groups, without modification of the stoichiometry of paclitaxel binding to tubulin. Moreover, 4 μM $As_2O_3$ inhibited the release of cytochrome *c* from isolated mitochondria by $78 \pm 10\%$. Our results show that $As_2O_3$ and paclitaxel act antagonistically on mitochondria and microtubules and illustrate the need for careful evaluation of drug combinations. 

*Keywords:* Drug combination; Tubulin; Cytochrome *c*; Antimicrotubule agents; Arsenic trioxide; Apoptosis

## 1. Introduction

Adverse health effects caused by arsenic compounds have long been recognized. Ingestion of large doses of arsenic may be acutely fatal. Chronic exposure to arsenic results in neurotoxicity, liver injury, peripheral vascular disease and an increased risk of cancer [1]. However, arsenic agents have been used as anticancer agents in traditional medicine [2]. In the 1970s, the effective component in the remedy was identified as $As_2O_3$. Recently, long-term clinical trials have indicated that low plasma concentrations of $As_2O_3$ (1–2 μM) are effective in the treatment of APL involving the translocation t(15:17) [3], even in patients resistant to all-*trans*-retinoic acid (ATRA) or conventional chemotherapy [4]. The translocation t(15:17), which fuses the *PML* gene on chromosome 15 to the *RARα* gene on chromosome 17, results in the expression of a PML-RARα chimeric protein. $As_2O_3$ induced its degradation [5] leading to the speculation that its expression was associated with the sensitivity to $As_2O_3$. More recently, it has been shown that 1 μM $As_2O_3$ induces apoptosis not only in APL cell lines but also in other leukemia cells without PML/RARα, in esophageal carcinoma, in neuroblastoma, in cervical carcinoma, and in prostate and ovarian carcinoma cell lines [6–10].

* Corresponding author. Tel.: +33-4-91-83-56-35; fax: +33-4-91-78-20-24.
*E-mail address:* diane.braguer@pharmacie.univ-mrs.fr (D. Braguer).

*Abbreviations:* APL, acute promyelocytic leukemia; PML, promyelocytic leukemia; RAR, retinoic acid receptor; PTP, permeability transition pore; DMSO, dimethylsulfoxide; MTS, 3-(4,5-dimethylthiazol-2-yl)-5-(3-carboxymethoxyphenyl)-2-(4-sulfophenyl)-2*H*-tetrazolium; CI, combination index; PI, propidium iodide; DAPI, 4,6-diamino-2-phenylindole; GTP, guanosine triphosphate; DTNB, 5,5′-dithiobis(2-nitrobenzoic acid); FLUTAX, 7-*O*-[*N*-(4′-fluoresceincarbonyl)-L-alanyl]taxol; VDAC, voltage-dependent anion channel; HSP, heat shock protein.

0006-2952/02/$ – see front matter 
PII: S0006-2952(02)00922-X

The mechanism whereby $As_2O_3$ targets the tumor cells is not clearly understood. Several lines of evidence suggest that $As_2O_3$ could act as a mitochondriotoxic agent. It induces an early transmembrane potential collapse that causes the release of cytochrome *c* from mitochondria to cytosol. $As_2O_3$ is able to act on isolated mitochondria to induce the opening of the PTP thus inducing apoptosis via a direct mitochondrial effect leading to caspase activation through release of pro-apoptotic factors [11]. Moreover, *ex vivo* studies on the APL cell line NB4 demonstrated that $As_2O_3$ down-regulates the expression of Bcl2, a protein located on the mitochondrial membrane, and induces apoptosis [12]. However, it cannot be ruled out that this agent may have additional effects that also contribute to cell death, because of its affinity for SH-groups present on numerous proteins [13]. Indeed, $As_2O_3$ may interfere with a staggering variety of cellular processes, e.g. cell cycle progression, DNA repair, tubulin polymerization, synthesis of reactive oxygen species synthesis and oncogene expression or activation [1,14–19].

Paclitaxel (Taxol®) is an anticancer drug highly efficacious in the treatment of breast, ovarian and lung malignancies [20] and is currently in evaluation for childhood tumors [21]. It is an antimicrotubule agent that stabilizes the microtubule network and inhibits microtubule dynamics [22]. Paclitaxel induces apoptosis after blockage at the metaphase–anaphase transition, Bcl2 phosphorylation, and subsequent cleavage of caspase-3 and poly(ADP ribose) polymerase. Its mechanism of action includes activation of a number of signal transduction pathways [23,24]. Moreover, it may also act via a mitochondrial pathway. Indeed, we have previously shown that the transmembrane potential was decreased simultaneously with activation of caspase-8 and caspase-3 during apoptosis induced by paclitaxel in proliferating colon cancer cells [25] and we have also found that paclitaxel directly affects mitochondria isolated from neuroblastoma cells resulting in release of cytochrome *c* [26].

Currently, the use of several antitumor agents in combination is under intense evaluation, particularly for the treatment of advanced or recurrent cancers refractory to standard chemotherapy. Many combination therapies now being tested use drugs that belong to different classes of anticancer drugs with the rationale that targeting two independent pathways will result in enhanced cytotoxicity, whether additive or synergistic. In addition, there are many trials of combination of agents with similar mechanisms of action or molecular targets. The pathways of apoptosis employed reflect not only the drug target but also the apoptotic machinery of the cell type. Finally, the efficacy of drug combinations also depends on drug resistance, and on the concentrations and schedules of treatment. The potential use of paclitaxel with conventional anticancer drugs, including microtubule depolymerizing agents, is currently being tested both *in vitro* and in clinical trials [27,28]. Numerous combinations of paclitaxel with less conventional agents have been investigated: P-glycoprotein inhibitors, trastuzumab, inhibitors of angiogenesis, inhibitors of epidermal growth factor receptor-associated tyrosine kinase, polyamine analogs, or lonidamine [29–35]. Combined $As_2O_3$ and ATRA treatment in APL leukemia induce complete clinical remission suggesting a possible therapeutic synergism [36,37]. Recently, the combinations of $As_2O_3$ with ascorbic acid [38] or with idarubicin [39] have been found synergistic in pilot clinical studies, and additive effects of $As_2O_3$ were demonstrated *in vitro* with cisplatin, adriamycin, and etoposide [10] suggesting that arsenic could be a potential new anticancer drug useful in several chemotherapy protocols.

This study is the first investigating the combination of arsenic and paclitaxel, both drugs being tested in the range of therapeutic concentrations. The study focuses on the effects of both $As_2O_3$ and paclitaxel on the microtubule network and on mitochondria. We used neuroblastoma cells because this malignant tumor of very early childhood has a very poor prognosis and remains a particularly difficult therapeutic challenge. The SK-N-SH cell line was chosen because we have previously demonstrated that paclitaxel induces apoptosis in this cell line and acts directly on isolated mitochondria from these cells [26,40,41]. First, we showed that therapeutic concentrations of $As_2O_3$ and paclitaxel added simultaneously were antagonistic to inhibition of proliferation of SK-N-SH cells using the CI method. Then, we found that both mitochondria and microtubules were involved in the mechanism of this antagonism by using *in vitro* systems.

## 2. Materials and methods

### 2.1. Cell culture

Human neuroblastoma SK-N-SH cells were routinely maintained at 37° and 5% $CO_2$, in standard culture RPMI-1640 medium (BioWhittaker) containing 10% fetal bovine serum (BioWhittaker), 2 mM glutamine, 1% penicillin and streptomycin. Exponentially growing cells ($10^5$ cells $mL^{-1}$) were seeded 3 days before drug treatment.

### 2.2. Drugs

$As_2O_3$ was obtained from Sigma and dissolved in 1 M NaOH. Stock solution of paclitaxel (Sigma) was prepared in DMSO. The highest final concentration of DMSO used in cell culture was 0.2%. Doxorubicin (Dakota) and vinblastine (Lilly) were prepared in aqueous solution. Tritiated paclitaxel (37 Ci/mmol) was obtained from Moravek.

### 2.3. Quantification of intracellular drug accumulation

Intracellular concentrations of arsenic were determined using atomic absorption spectrophotometry after digestion

with nitric acid. Three independent experiments were performed after treatment of cells with 5 μM $As_2O_3$ for 6 hr. Cellular incorporation of paclitaxel was measured as previously described [42]. We first measured the kinetics of paclitaxel uptake to determine the time of drug incubation to attain steady-state levels. Exponentially growing cells were then exposed to 200 nM of [$^3$H]-paclitaxel for 4 hr. Cells were then harvested, washed several times in phosphate buffer and lysed in 60% methanol. Cell lysate was counted for radioactivity by liquid scintillation counting (LS1707, Beckman). Concentration of intracellular paclitaxel was calculated using [$^3$H]-paclitaxel standards.

To estimate the cell volume, the diameters of trypsinized cells were measured under electronic and optical microscopes with a micrometer. These data were confirmed by estimation of the cellular diameters by flow cytometry using calibrated glass beads (2 and 6 μm).

### 2.4. Cytotoxicity assays

Growth inhibition of SK-N-SH cells was studied following a 72-hr treatment with drugs by using the MTS reagent of the CellTiter 96 $AQ_{ueous}$ nonradioactive cell proliferation assay (Promega) with absorption measured at 490 nm. The $IC_{50}$ values were first established for each drug separately. Then, combinations of $As_2O_3$ with the other anticancer drugs were evaluated for synergy, additivity, or antagonism using the CI method of Chou and Talalay [43] and the computer program Calcusyn software (Biosoft). The constant drug ratios examined were based on the ratio of the $IC_{50}$ of the individual drugs. The combination index (CI) is defined as: $CI = (D)_1/(D_x)_1 + (D)_2/(D_x)_2 + \alpha(D)_1(D)_2/(D_x)_1(D_x)_2$, where $\alpha = 0$ for drugs with mutually exclusive mechanisms of action (similar mechanism of action), $\alpha = 1$ for drugs with mutually nonexclusive mechanisms, $(D)_1$ is the dose of drug 1, $(D)_2$ is the dose of drug 2, and $(D_x)$ is the dose required to cause a median effect. Median effect plots were used [log(dose) vs. log(fraction of cells affected/fraction not affected)] to determine the appropriate model for analysis of the drug combination. In our study, the lines obtained for the drugs alone and in combination were not parallel, leading to an evaluation based on a nonexclusive effect. CI values <1 or >1 indicate synergism or antagonism, respectively, whereas a value of 1 indicates additivity. Each data point is the mean ± SD of at least three independent experiments, each of which was performed in triplicate.

Cell growth measurements were confirmed by using Trypan blue exclusion method. After drug treatment, supernatant and adherent cells were collected and incubated with 0.4% Trypan blue in phosphate-buffered saline for 5 min at 37° and the number of stained (non-viable) and unstained (viable) cells were counted. Cell viability was expressed as the percent ratio of unstained cells vs. the total number of cells.

### 2.5. Detection of apoptosis by Annexin-V-FITC and DAPI staining

Surface exposure of phosphatidylserine in apoptotic cells was measured by using Annexin-V-FITC (Euromedex) as described previously [25,40]. Following a 72-hr paclitaxel and/or $As_2O_3$ treatment, supernatant and adherent cells were exposed to Annexin-V-FITC and PI for 15 min before flow cytometry analysis (FACScan, Becton Dickinson) [40]. Apoptosis was also detected by DAPI staining (Sigma) as previously described [44], and the percentages of cells in interphase, mitosis and apoptosis were quantified. Apoptotic cells were defined by the condensation of nuclear chromatin and nuclear fragmentation.

### 2.6. Cell cycle analysis by flow cytometry

After drug treatment, cells were harvested, fixed in cold methanol and incubated with propidium iodide immediately before analysis. DNA content was measured by flow cytometry as previously described [28].

### 2.7. Visualisation of microtubular network by immunofluorescence microscopy

After treatment with paclitaxel and/or $As_2O_3$ for 72 hr, cells were fixed with formaldehyde 3.7% and permeabilized with saponin (0.1%). Immunofluorescence microscopy of the microtubule network was performed using α-tubulin antibody (Amersham) and an FITC-conjugated secondary antibody (Sigma) as described [41].

### 2.8. Tubulin polymerization assays

Tubulin was purified from pig brains by ammonium sulfate fractionation and ion exchange chromatography [45]. Protein concentrations were determined spectrophotometrically with an extinction coefficient $\varepsilon_{275\,nm} = 1.09\ L\ g^{-1}\ cm^{-1}$ in 6 M guanidine hydrochloride. Purified tubulin 6S was equilibrated in 20 mM sodium phosphate buffer pH 6.7, 1 mM EGTA, 3.4 M glycerol, 0.1 mM GTP, as previously described [46]. Tubulin (1.5 mg $mL^{-1}$) was preincubated 1 hr at 37° with $As_2O_3$ (5–200 μM). Microtubule assembly was initiated by adding 10 mM $MgCl_2$ at 37° in thermostated cuvettes, and the mass of polymer formed was monitored by turbidimetry at 350 nm with a Beckman DU7400 spectrophotometer. For experiments with the combination of paclitaxel and $As_2O_3$, paclitaxel at concentration equimolar with tubulin (15 μM) was added with the $MgCl_2$. Samples were taken at the end of polymerization time and then negatively stained with 2% uranyl acetate on formvar coated grids as described previously [44]. The structure of microtubules was visualized by using transmission electron microscopy (JEOL 1220).

### 2.9. Determination of tubulin SH group concentration

Determination of tubulin-free SH groups was performed by using DTNB (Sigma). After $As_2O_3$ preincubation at 37° for 1 hr, 0.1 mL of tubulin solution was mixed to 0.9 mL of a buffer containing 20 mM NaPi, pH 7.5, 6.4 M urea, and 1 mM DTNB. The formation of a thio-nitrobenzoate anion induced by DTNB reaction with free SH groups of tubulin was monitored by measuring absorbance at 412 nm, and the SH group concentration was calculated using $\varepsilon_{412\,nm} = 13{,}600\ M^{-1}\ cm^{-1}$. The time course of the effect of 200 μM $As_2O_3$ was determined from 1 to 24 hr; concentrations of $As_2O_3$ ranged from 10 to 200 μM (1-hr preincubation).

### 2.10. Measurement of stoichiometry of paclitaxel binding to microtubules

Purified tubulin was preincubated at 37° for 1 hr in presence or absence of 200 μM $As_2O_3$ in 20 mM sodium phosphate buffer pH 6.7, 1 mM EGTA, 3.4 M glycerol, 0.1 mM GTP. Then, polymerization was initiated by adding 7 mM $MgCl_2$ and the fluorescent paclitaxel FLUTAX I in a 1.2:1 taxoid–tubulin molar ratio, and tubulin was assembled at 37° for 2 hr, as described by Andreu [47]. After centrifugation, pellets of microtubules were resuspended in cold 20 mM sodium phosphate buffer pH 7.0, 1 mM EGTA, 3.4 M glycerol, 7 mM $MgCl_2$, and 0.25% SDS. Determination of SH group concentration of assembled tubulin was performed to check whether microtubules formed were modified by $As_2O_3$. Then, tubulin and FLUTAX I concentrations in pellets were determined spectrophotometrically, employing $\varepsilon_{275\,nm} = 107{,}000\ M^{-1}\ cm^{-1}$ [46] and $\varepsilon_{458\,nm} = 23{,}100\ M^{-1}\ cm^{-1}$, respectively [47] (a new determination gave essentially the same value). The concentration of FLUTAX I in supernatants was measured fluorometrically using $\lambda_{ex} = 470$ nm and $\lambda_{em} = 522$ nm to ensure that ligand in excess remained in the supernatant.

### 2.11. Isolation of mitochondria and Western blot analysis of mitochondrial proteins

Mitochondria were isolated from SK-N-SH cells as described [27]. Isolated mitochondria were aliquoted and incubated for 2 hr at 37° with 0.02% DMSO and/or NaOH (0.3 μM) (control), 100 μM paclitaxel, 4 μM $As_2O_3$, or the combination of the two drugs. After centrifugation (15,000 *g*), pellets and supernatants were carefully separated, mitochondrial pellets were lysed and Western blot analysis of cytochrome *c* was performed as described [26]. VDAC antibody (Calbiochem) was used to ensure that equal amounts of mitochondrial proteins were loaded and that no mitochondria remained in the supernatant. Detection of tubulin in mitochondrial and total cellular lysates was performed using α-tubulin (Amersham) and β-tubulin (Sigma) antibodies. Quantification was performed as previously described [26,28].

## 3. Results

### 3.1. $As_2O_3$ reduced the paclitaxel-induced inhibition of SK-N-SH cell proliferation

$As_2O_3$ inhibited proliferation of SK-N-SH cells in a time- and concentration-dependent manner. At 72-hr treatment, the $IC_{50}$ of $As_2O_3$, i.e. the concentration inhibiting 50% of cell proliferation, was 8 μM, as shown in Fig. 1A. SK-N-SH cells were sensitive to paclitaxel as shown previously [41]. Paclitaxel (100 nM) inhibited 50% of the cell proliferation at 72 hr of treatment (Fig. 1B). The percentage of viable cells was increased by $35 \pm 4$ and $60 \pm 3\%$ ($P < 0.01$) when cells were treated with $As_2O_3$ (1 and 5 μM, respectively) simultaneous with treatment with paclitaxel 100 nM (Fig. 1C). In the same experimental conditions, a decrease in paclitaxel-cell death ($38 \pm 3$ and $50 \pm 6\%$ with 1 and 5 μM $As_2O_3$, respectively) was measured by using the Trypan blue exclusion technique. All these data suggested that the combination might be antagonistic. CI values for the simultaneous combination of paclitaxel and $As_2O_3$ in a ratio of 1:80 varied from $3.4 \pm 0.4$ to $36.7 \pm 2.6$ for combination concentrations from 12.5 nM paclitaxel:1 μM $As_2O_3$ to 400 nM paclitaxel:32 μM $As_2O_3$. These CI values, considerably higher than 1, confirmed the strong antagonistic drug interaction.

In order to specify the mechanism of this antagonism, subsequent experiments at the cellular level were performed with 200 nM paclitaxel, twice the $IC_{50}$ value, and 1 μM $As_2O_3$, the concentration of drug alone that induced no significant effect on SK-N-SH cells. In these experimental conditions, $As_2O_3$ did not affect the intracellular concentration of paclitaxel ($55 \pm 11$ μM).

### 3.2. $As_2O_3$ decreased paclitaxel-induced apoptosis

Cell cycle analysis by flow cytometry confirmed the reduction in cell death following a 72-hr treatment with the combination of 200 nM paclitaxel and 1 μM $As_2O_3$ compared with 200 nM paclitaxel alone ($48 \pm 3$ and $75 \pm 5\%$, respectively). To investigate whether the lower cytotoxicity induced by the combination was due to a decrease in apoptosis, we performed DAPI and Annexin-V-FITC staining. By using DAPI staining, we determined that 1 μM $As_2O_3$ significantly decreased paclitaxel-induced apoptosis by $40 \pm 5\%$ ($P < 0.01$). This decrease in apoptotic cells was further confirmed by Annexin-V-FITC staining as mentioned in Table 1.

### 3.3. $As_2O_3$ specifically antagonized inhibition of proliferation induced by antimicrotubule drugs

We investigated whether the antagonistic effect of $As_2O_3$ also occurred in combination with vinblastine, another antimicrotubule agent, or with doxorubicin, a drug whose mechanism of action is independent of microtubules (Fig. 2).

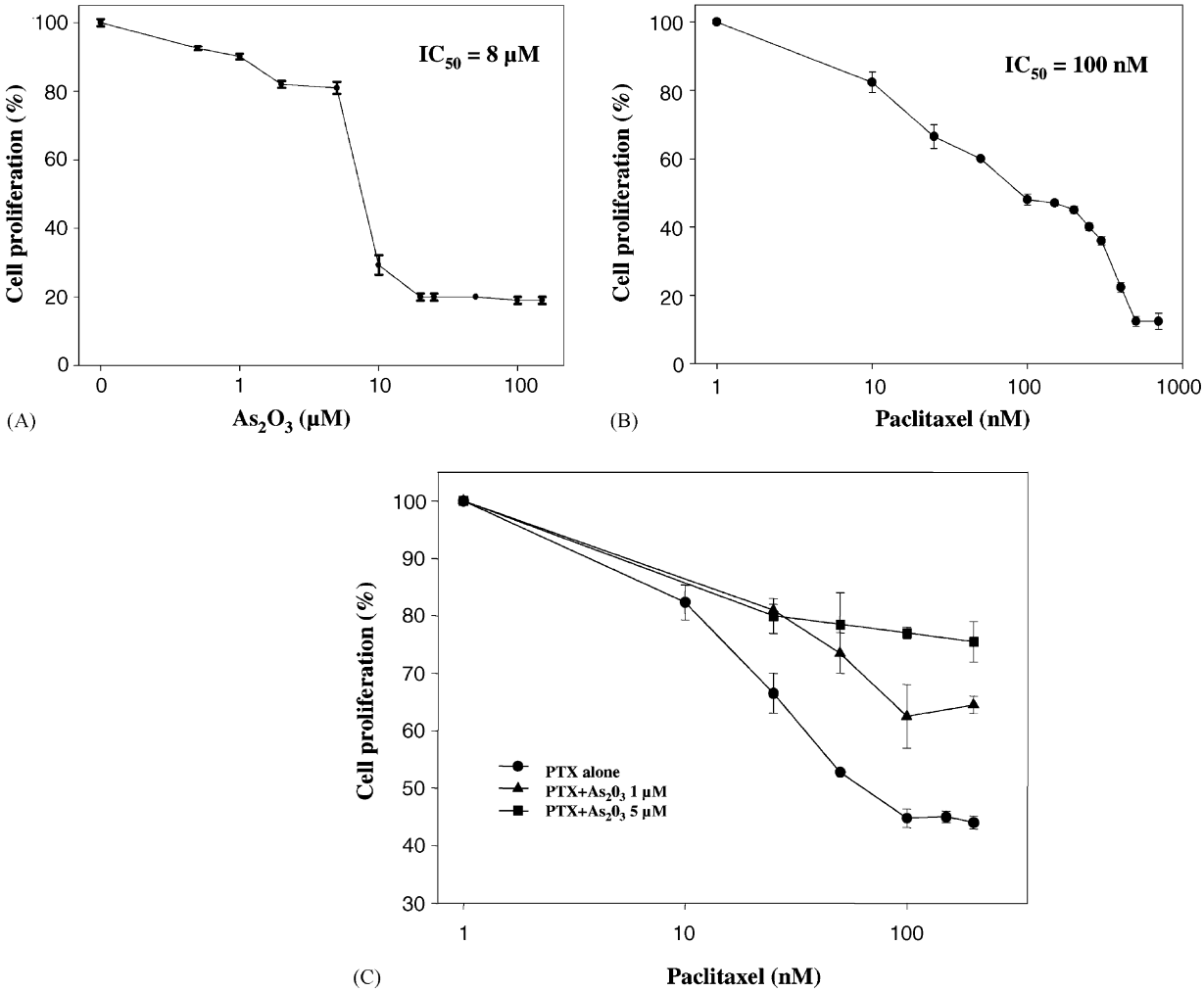


Fig. 1. $As_2O_3$ decreased paclitaxel (PTX) cytotoxicity. Cytotoxicity of (A) $As_2O_3$ alone, (B) paclitaxel alone, or (C) combined drugs. Exponentially growing cells were treated with the indicated concentrations of paclitaxel and/or $As_2O_3$ for 72 hr, and cell proliferation was assessed by using the MTS reagent (see Section 2). The data represent the mean ± SD of at least three independent experiments in triplicate.

Measurements of cytotoxicity showed that $As_2O_3$ decreased inhibition of cell proliferation induced by vinblastine alone. Vinblastine (10 nM) induced $45 \pm 2\%$ inhibition of cell proliferation, whereas 10 nM vinblastine in combination with 1 or 5 µM $As_2O_3$ induced only $35 \pm 4$ or $25 \pm 1\%$ inhibition of cell proliferation, respectively (Fig. 2A). The CI values were much higher than 1 (as high as $7.9 \pm 0.3$; data not shown), demonstrating that vinblastine and $As_2O_3$ are antagonistic. In contrast, no significant change in the percentage of inhibition of cell proliferation was observed between treatment (72 hr) with doxorubicin alone or in combination with $As_2O_3$ (1 and 5 µM) (Fig. 2C). Moreover, CI values were approximately 1, confirming that doxorubicin and $As_2O_3$ were not antagonistic (data not shown).

### 3.4. $As_2O_3$ antagonized the effects of paclitaxel on microtubules

Since $As_2O_3$ specifically antagonized the cytotoxicity of antimicrotubule drugs, we investigated whether the interaction between paclitaxel and $As_2O_3$ occured at microtubule level. Antimicrotubule agents generally induce mitotic block in proliferating cells. Thus, we investigated by cell cycle analysis whether $As_2O_3$ could modify the mitotic block induced by paclitaxel. A 24-hr treatment with the combination of paclitaxel (200 nM) and $As_2O_3$ (1 µM) decreased by $20 \pm 2\%$ ($P < 0.01$) the number of

Table 1
$As_2O_3$ decreased paclitaxel-induced apoptosis

| | Apoptotic cells (%) | |
|---|---|---|
| | PTX 200 nM | PTX 200 nM + $As_2O_3$ 1 µM |
| Cell cycle analysis | $75 \pm 5$ | $48 \pm 3$ |
| DAPI staining | $70 \pm 1$ | $43 \pm 4$ |
| Annexin-V staining | $72 \pm 3$ | $52 \pm 6$ |

Quantification of apoptotic SK-N-SH cells (% ± SD) was performed by cell cycle analysis, DAPI and Annexin-V staining after incubation for 72 hr with paclitaxel or with the combination of paclitaxel plus $As_2O_3$. For the DAPI method, percentages of apoptotic cells were determined in a population of 500 cells in three independent experiments.

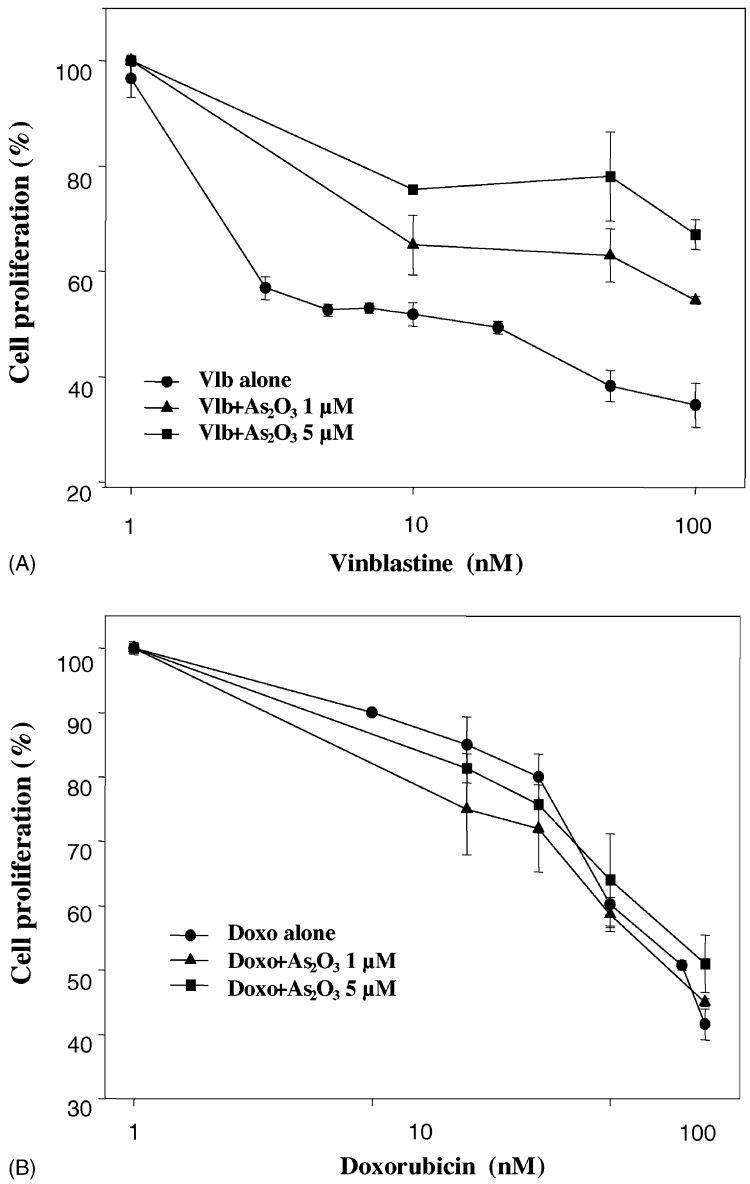


Fig. 2. $As_2O_3$ decreased the cytotoxicity of vinblastine (Vlb) but not doxorubucin (Doxo). Cytotoxicity of (A) vinblastine or (B) doxorubicin alone and in combination with $As_2O_3$. Exponentially growing cells were treated with the indicated concentrations of vinblastine or doxorubicin and $As_2O_3$ for 72 hr, and cell proliferation was assessed by using the MTS reagent (see Section 2). The data represent the mean ± SD of at least three independent experiments in triplicate.

cells blocked in G2/M phase, compared with paclitaxel alone (Fig. 3). To examine the actions of $As_2O_3$ and paclitaxel in combination on the microtubule network, we performed comparative immunostaining of α-tubulin in control cells, and in cells treated with 200 nM paclitaxel alone, with 1 µM $As_2O_3$ alone, or with the combination at the same concentrations for 6 hr. $As_2O_3$ alone did not induce changes in the appearance of the microtubule network (Fig. 4B). However, microtubule bundles, which are classically detected following paclitaxel treatment (Fig. 4C), appeared less condensed following treatment with the drug combination (Fig. 4D).

We examined the combined effect of $As_2O_3$ and paclitaxel on microtubule assembly *in vitro*. $As_2O_3$ inhibited formation of microtubules from tubulin 6S in a concentration-dependent manner, from 10 to 200 µM $As_2O_3$ (Fig. 5A). The decrease in turbidity observed following a drop in temperature at 10° indicates that the structures formed in presence of $As_2O_3$ were microtubules and not aggregates. Polymerization of tubulin by paclitaxel was inhibited by $As_2O_3$ in a concentration-dependent manner (5–200 µM) (Fig. 5D). Electron microscopy confirmed the formation of microtubules in all of the conditions (Fig. 5B, C, E and F). Altogether, these results indicate that $As_2O_3$ antagonizes the effects of paclitaxel on microtubule assembly.

In order to examine how paclitaxel and $As_2O_3$ interact on tubulin, we first examine the binding of $As_2O_3$ on

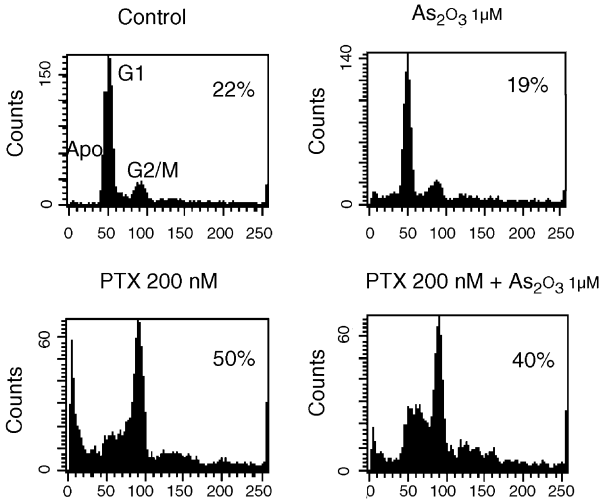


Fig. 3. $As_2O_3$ caused a decrease in the G2/M-phases block induced by paclitaxel. SK-N-SH cells were untreated or incubated with either 1 μM $As_2O_3$, 200 nM paclitaxel, or the combination of the two drugs for 24 hr. Cells were fixed, stained with propidium iodide, and analysed by flow cytometry as described in Section 2. Percentage of G2/M arrested cells is noted. Data are representative of three independent experiments.

tubulin SH groups [13]. $As_2O_3$ (200 μM) decreased the percentage of free SH groups of tubulin in a time-dependent manner ($10 \pm 1\%$ of free SH groups remained following a 24-hr incubation; data not shown). The decrease in free SH groups of tubulin was concentration-dependent and was correlated to inhibition of polymerization ($r = 0.987$) (Table 2A). Thus, $As_2O_3$ binds to tubulin SH groups which modifies the conformation of tubulin and consequently inhibits its polymerization, as novel classes of agents can do [48,49]. We then investigated whether $As_2O_3$ could affect the binding of paclitaxel on tubulin by using the fluorescent paclitaxel FLUTAX I. Measurement of the FLUTAX binding stoichiometry indicated that the number of molecules of paclitaxel bound per assembled tubulin dimer was identical in the presence and in the absence of $As_2O_3$ ($P > 0.05$) (Table 2B). Thus, the stoichiometry of paclitaxel binding was not modified by the interaction of $As_2O_3$ with tubulin SH groups.

### 3.5. $As_2O_3$ antagonizes the effects of paclitaxel at mitochondrial level

$As_2O_3$ has been generally described as a mitochondriotoxic agent [11]. We have recently shown that paclitaxel acted on mitochondria isolated from SK-N-SH cells to release cytochrome *c* [26]. Thus, we investigated the effect of $As_2O_3$ alone and combined with paclitaxel on the release of cytochrome *c* (Fig. 6A). Expression of VDAC was systematically measured to ensure that equal amounts of mitochondrial proteins were loaded onto the gels and that

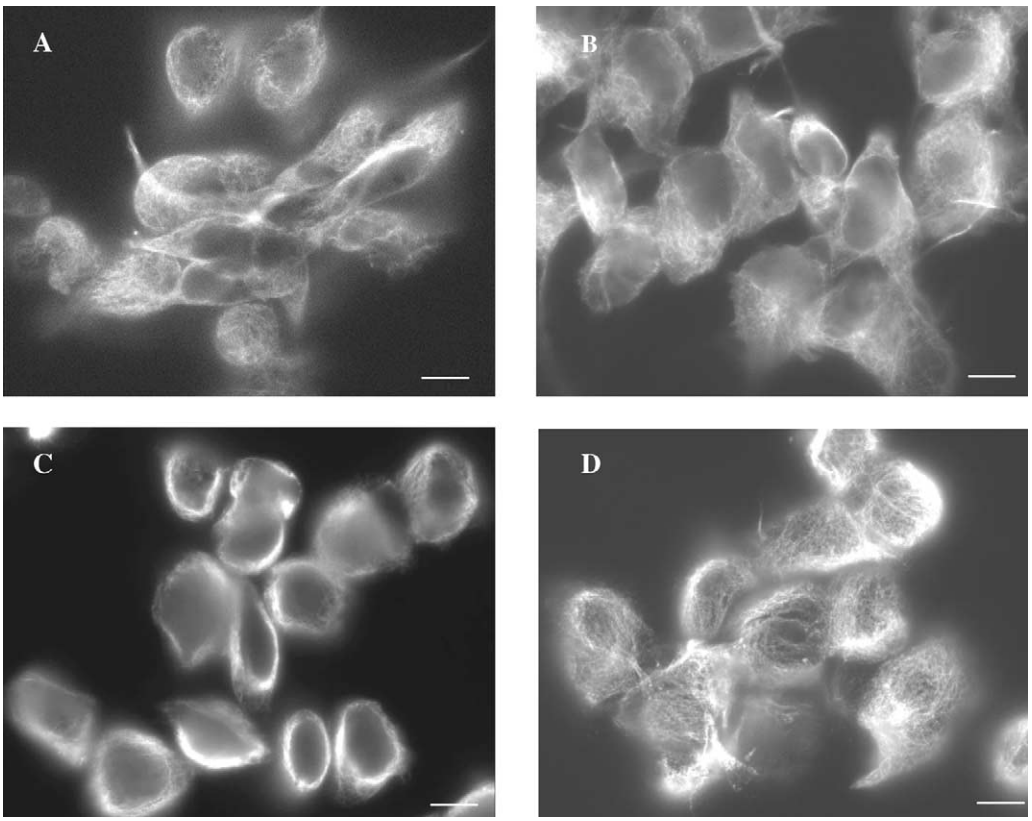


Fig. 4. $As_2O_3$ inhibited formation of bundles induced by paclitaxel. SK-N-SH cells were (A) untreated or treated for 6 hr with (B) 1 μM $As_2O_3$, (C) 200 nM paclitaxel, or (D) the combination of the two drugs, and microtubules were immunostained with an α-tubulin antibody as described in Section 2. Scale bar: 5 μm.

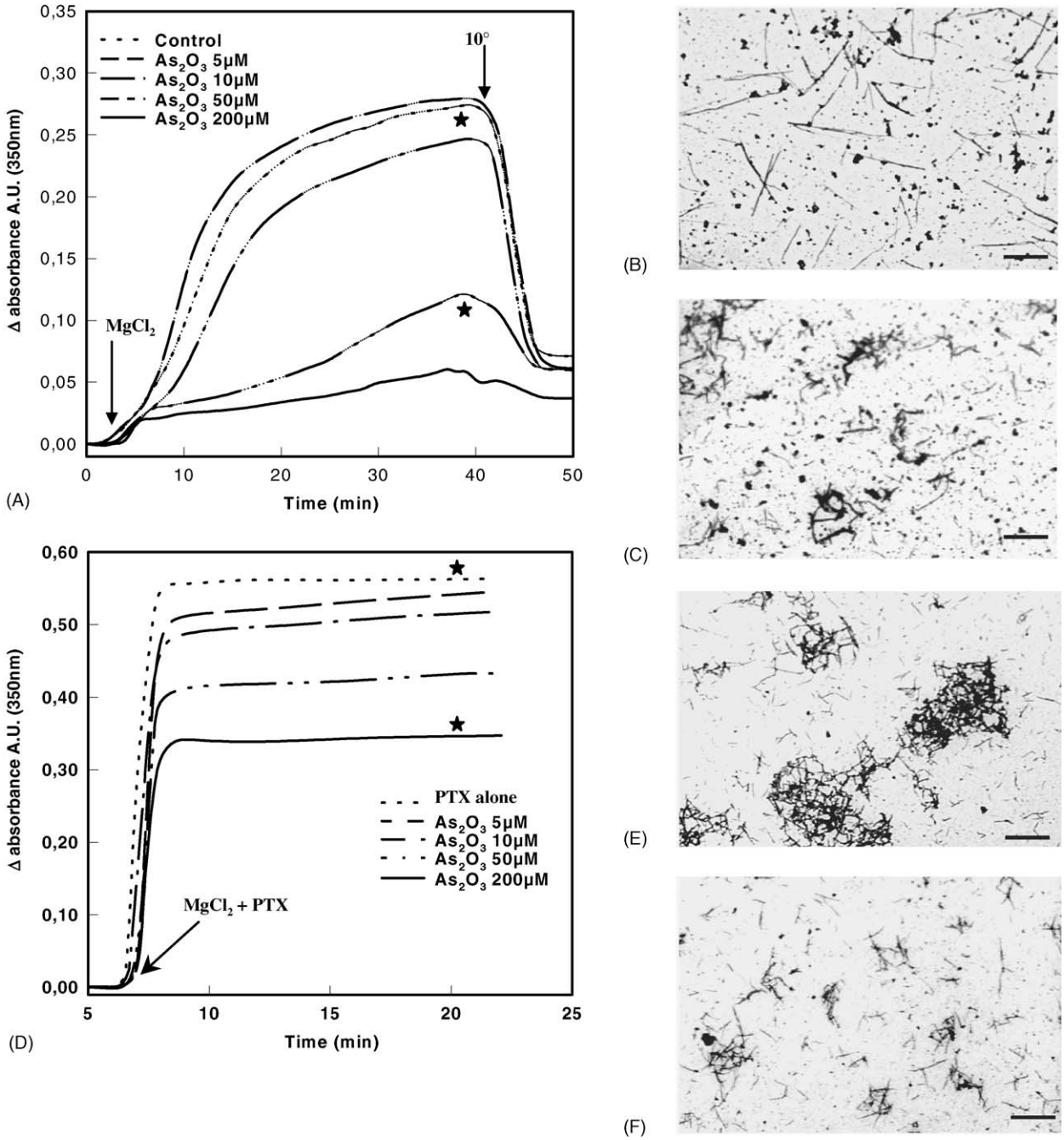


Fig. 5. $As_2O_3$ inhibited tubulin polymerization *in vitro*, even in presence of paclitaxel. Purified tubulin 6S (1.5 mg $mL^{-1}$) was preincubated with $As_2O_3$ (0–200 μM) for 1 hr at 37° in a $MgCl_2$-free buffer. Polymerization was then started by adding (A) 10 mM $MgCl_2$ alone or (D) simultaneously with 15 μM paclitaxel, and formation of microtubules was determined by measuring turbidimetry ($A_{350\ nm}$). Data are representative of three independent experiments. Visualization by transmission electron microscopy of microtubules (B) in the control sample (without paclitaxel or $As_2O_3$), and formed in presence of (C) 50 μM $As_2O_3$, (E) 15 μM paclitaxel alone, or (F) combination of 15 μM paclitaxel and 200 μM $As_2O_3$. Samples for electron microscopy were prepared when the plateau of polymerization was reached (indicated by a star) as described in Section 2. Scale bar: 5 μm.

no mitochondria remained in the supernatant. $As_2O_3$ (4–1000 μM) induced a release of cytochrome *c* (data not shown). Then, the combination of $As_2O_3$ and paclitaxel was tested at concentrations reflecting the intracellular concentrations inducing apoptosis. For this purpose, we determined the intracellular content of arsenic by atomic absorption spectrophotometry. After treatment with 5 μM of $As_2O_3$ for 6 hr, the final concentration of arsenic in the cells was estimated to be 20 μM, indicating that $As_2O_3$ was 4-fold concentrated into the cells. This result is in agreement with measurement of intracellular arsenic described in HeLa cells [50]. Intracellular paclitaxel concentration reached more than 100 μM (data not shown) and we have previously shown that 100 μM paclitaxel-induced release of cytochrome *c* from mitochondria isolated from SK-N-SH cells [26]. Thus, isolated mitochondria were treated for

Table 2
$As_2O_3$ interacted with free SH groups of tubulin without modifying the stoichiometry of paclitaxel binding

A

| $As_2O_3$ concentration (μM) | Tubulin-free SH groups (%) | Tubulin polymerization (%) |
|---|---|---|
| 0 | 100 | 100 |
| 10 | 92 ± 2 | 81 ± 4 |
| 50 | 83 ± 2 | 43 ± 1 |
| 200 | 78 ± 1 | 16 ± 2 |

B

| | Flutax 10 μM | Flutax 10 μM + $As_2O_3$ 200 μM |
|---|---|---|
| Flutax—microtubules stochiometry | 0.85 ± 0.06 | 0.89 ± 0.05 |
| Microtubule-free SH groups (%) | 100 | 79 ± 2 |

(A) Dose dependent interaction of $As_2O_3$ with tubulin SH groups was related with inhibition of tubulin polymerization by $As_2O_3$. Percentages of free SH groups were determined by using DTNB as described in "Material and Methods".

(B) Stoichiometry of fluorescent paclitaxel binding to tubulin was not modified by interaction of 200 μM $As_2O_3$ with microtubule SH groups. The values of stoichiometry represent the number of fluorescent paclitaxel molecules bound per assembled tubulin dimer. Data represent the mean ±SD of at least three independent experiments.

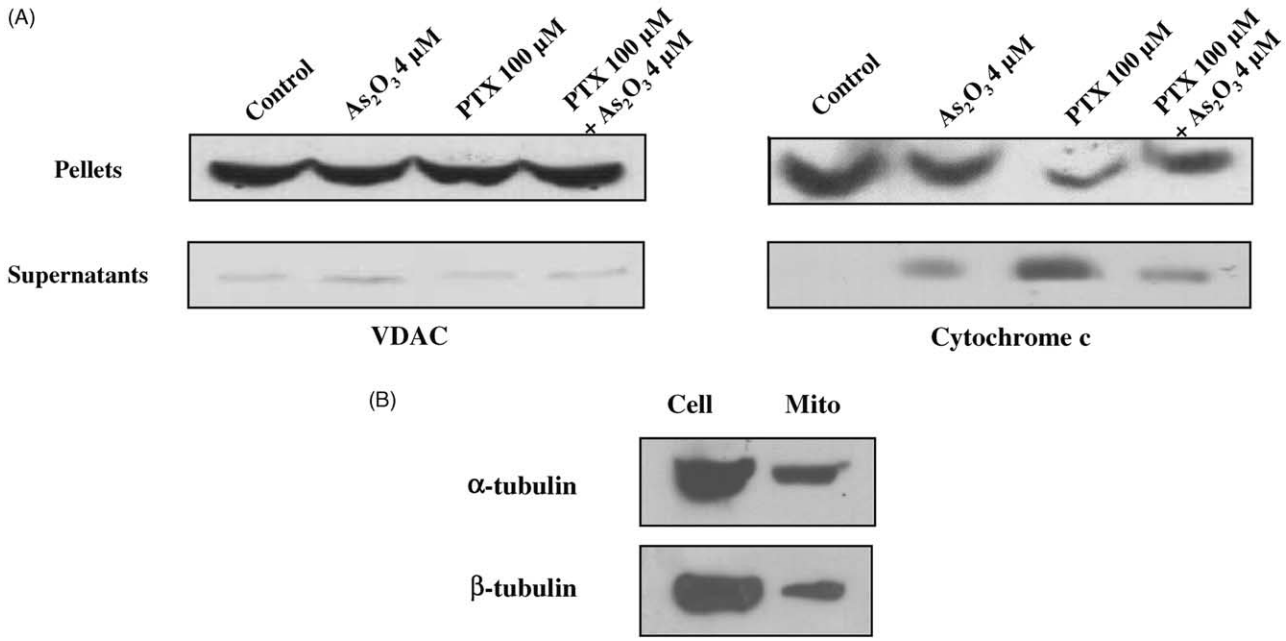


Fig. 6. $As_2O_3$ inhibited release of cytochrome *c* induced by paclitaxel. (A) Isolated mitochondria from SK-N-SH cells were incubated with $As_2O_3$, paclitaxel, or the combination of the two drugs for 2 hr at 37°. Supernatants and mitochondrial lysates were analysed by immunoblotting using cytochrome *c* antibody. Gel loading equivalence and absence of mitochondria in the supernatants were confirmed by reprobing with antibody to VDAC. (B) The presence of tubulin on isolated mitochondria was examined by immunoblotting with α- and β-tubulin antibodies. Data are representative of at least three independent experiments.

2 hr with 4 μM $As_2O_3$ and 100 μM paclitaxel alone and in combination. As shown on Fig. 6A, paclitaxel and $As_2O_3$ each induced cytochrome *c* release. However, when combined the quantity of cytochrome *c* released by the combination was 78 ± 10% lower than the quantity released by paclitaxel alone ($P < 0.01$). The same reduction also occurred when $As_2O_3$ was increased to 30 μM in the combination (data not shown). Thus, we conclude that $As_2O_3$ antagonizes paclitaxel's effect at the mitochondrial level. As shown on Fig. 6B, tubulin dimers (α,β-tubulin) are localized on mitochondria, suggesting that both paclitaxel and $As_2O_3$ may trigger cytochrome *c* release through an action on mitochondrial tubulin.

## 4. Discussion

We found that the simultaneous combination of $As_2O_3$ and paclitaxel in the therapeutic concentration range is antagonistic on proliferation of neuroblastoma cells, and they act at both mitochondrial and microtubular levels, as shown by using *in vitro* systems.

We first demonstrated that $As_2O_3$ was cytotoxic on SK-N-SH cells, thus, adding this cell line to the panel of neuroblastoma cell lines sensitive to $As_2O_3$ [8,51]. $As_2O_3$ antagonized the cytotoxicity of paclitaxel, as confirmed by median effect analysis using the CI method of Chou and Talalay, leading to a decrease in apoptotic cells. This antagonistic interaction was effective at clinically achievable concentrations [3,21].

Paclitaxel acts both on mitochondria [26] and microtubules [22]. Arsenic compounds act on mitochondria [11] and also disturb mitotic spindle formation, cell cycle progression and chromosome segregation [14,18,52], suggesting that they could interact with microtubules. Thus, we focused our study on the interaction of paclitaxel with $As_2O_3$ on isolated mitochondria and on tubulin. The effects of arsenic compounds on tubulin polymerization were investigated previously in several studies but there is disagreement among the results [18,50,52]. In the current study, turbidimetry and electron microscopy studies indicated that $As_2O_3$ induced a concentration-dependent inhibition of tubulin polymerization, 200 μM inducing an almost complete inhibition. Moreover, the depolymerizing effect of $As_2O_3$ was maintained even with paclitaxel. Thus, $As_2O_3$ is an inhibitor of tubulin polymerization and also inhibits paclitaxel-induced microtubule formation. The decrease in free SH groups of tubulin following $As_2O_3$ incubation was correlated with the inhibition of tubulin polymerization, suggesting that tubulin conformation was modified by interaction of $As_2O_3$ with vicinal SH groups. As the paclitaxel binding site does not contain SH groups, $As_2O_3$ cannot be a competitive inhibitor of paclitaxel binding to tubulin. Moreover, the stoichiometry of paclitaxel binding to tubulin was not modified in the presence of $As_2O_3$. Thus, the inhibition of paclitaxel-mediated microtubule assembly by $As_2O_3$ is not due to decreased binding of paclitaxel to tubulin. Through its action on SH groups, $As_2O_3$ certainly induces a conformational change of tubulin which results in a lower capacity of this tubulin to polymerize, even in presence of paclitaxel. The immunofluorescence microscopy studies support the *in vitro* polymerization assay; indeed, the combination induced disorganized bundles suggesting that $As_2O_3$ prevented paclitaxel from achieving its maximum activity. Antagonism observed at microtubular level may be also involved in the decrease in mitotic block, leading to a decrease in apoptotic cells co-treated with paclitaxel and $As_2O_3$, compared with cells treated with paclitaxel alone.

Release of cytochrome *c* from mitochondria is a key event in activation of apoptosis: cytochrome *c* binds to apaf-1 and pro-caspase 9, leading to activation of the apoptosome in the presence of ATP and subsequent apoptotic cascade of caspases, finally resulting in poly(ADP ribose) polymerase degradation and DNA cleavage. We previously found that paclitaxel was able to release cytochrome *c* from isolated mitochondria from SK-N-SH in a PTP-dependent manner [26]. In the current study, we have shown that $As_2O_3$ also induced release of cytochrome *c* from isolated mitochondria, thus confirming that $As_2O_3$ released mitochondrial factors to induce apoptosis [11]. Moreover, the combination of $As_2O_3$ and paclitaxel released approximately 80% less cytochrome *c* than was released by paclitaxel alone. This result on mitochondria may explain the antagonism of $As_2O_3$ on paclitaxel's effect. It may also explain in part the decrease in apoptotic cells following treatment with the combination. Interpretation of these data is difficult because the mechanism of cytochrome *c* release is not currently known, and both drugs have several potential targets at the mitochondrial level. Either the two drugs bind on common or adjacent sites, so that the drugs compete for their binding, or the two drugs have unrelated binding sites but the binding of one drug may modify the conformation of the other drug target's or the conformation of PTP through membranous proteins, thus leading to an alteration of its function. The adenine nucleotide translocator (ANT) is a protein of the PTP containing vicinal SH groups [53] and it was recently shown to be a target of $As_2O_3$ [54]. The mitochondrial antiapoptotic protein Bcl2 is also a potential candidate for paclitaxel binding [55] and for $As_2O_3$ binding since it contains SH groups. Moreover, both drugs interact with tubulin, and tubulin is expressed on mitochondrial membranes, suggesting that tubulin could also be a common target involved in the antagonism. As the amount of cytochrome *c* released by $As_2O_3$ was approximately the same in presence and in absence of paclitaxel, interaction of paclitaxel with the mitochondrial tubulin might be impeded by $As_2O_3$.

From all these results, it is tempting to consider $As_2O_3$ as an antimicrotubule agent, as suggested previously by Li and Broome [18]. However, other mechanisms shown on hematological cell lines [14] such as deregulation of cell cycle related-proteins also leading to mitotic disturbance and subsequent alteration in chromosome segregation could be involved in this antagonism. $As_2O_3$ has also the ability to induce *HSP* gene expression [56]. HSP70 protects cultured cells from apoptosis [57] by interfering with Apaf-1 or with the apoptosis inducing factor (AIF) [58,59]. Thus, HSP70 also could participate in the decrease of paclitaxel-induced apoptosis by $As_2O_3$. The decrease in respiration rate of cells treated with $As_2O_3$ (data not shown) could also be involved. Induction of differentiation has been described as a possible mechanism of action of $As_2O_3$ and it may be the rationale for therapeutic use in leukemia resistant to ATRA. However, $As_2O_3$-induced differentiation is probably not involved in the mechanism of antagonism we observed at 1 μM $As_2O_3$ because morphological features of differentiation such as neurites were only detected at 5 μM $As_2O_3$ (data not shown).

This study illustrates the complexity of analyzing drug combinations. Paclitaxel has one major target, the β-tubulin subunit in the microtubule. Binding of paclitaxel to β-tubulin in microtubules leads to several effects such as inhibition of microtubule dynamics, stabilization of

microtubules, formation of bundles of microtubules and activation of a number of signal transduction pathways. Conversely, $As_2O_3$ has several targets that are proteins with SH groups, thus suggesting several mechanisms of action for this drug. Our results clearly indicate antagonism, whereas such a combination might have predicted to act synergistically, demonstrating that it may be very hazardous to predict the final effect of a combination.

In conclusion, we have demonstrated that the simultaneous combination of $As_2O_3$ with paclitaxel was antagonistic at mitochondrial and microtubular levels. This result requires cautious interpretation and needs further work to determine whether this antagonism occurs whatever the modalities of combination, the concentrations and the cell type.

## Acknowledgments

The authors thank Vincent Peyrot and Mary Ann Jordan for helpful discussions, José Manuel Andreu for the gift of FLUTAX I, Pierre Rebouillon for measurements of intracellular concentrations of $As_2O_3$, Gaël Brasseur and Danielle Lemesle-Meunier for respiration rate experiments, Charles Prevôt for flow cytometric measurements, and the department of electron microscopy in the Faculty of Medicine (Marseille, France). NA received a fellowship from ARC (Association pour la Recherche sur le Cancer).

## References

[1] Chen YC, Lin-Shiau SY, Lin JK. Involvement of reactive oxygen species and caspase 3 activation in arsenite-induced apoptosis. J Cell Physiol 1998;177:324–33.

[2] Jiang S. Encyclopedia of chinese medecine. Shangia, China: Scientific Publishing House, 1986. p. 1620–2.

[3] Dai J, Weinberg RS, Waxman S, Jing Y. Malignant cells can be sensitized to undergo growth inhibition and apoptosis by arsenic trioxide through modulation of the glutathione redox system. Blood 1999;93:268–77.

[4] Shen ZX, Chen GQ, Ni JH, Li XS, Xiong SM, Qiu QY, Zhu J, Tang W, Sun GL, Yang KQ, Chen Y, Zhou L, Fang ZW, Wang YT, Ma J, Zhang P, Zhang TD, Chen SJ, Chen Z, Wang ZY. Use of arsenic trioxide ($As_2O_3$) in the treatment of acute promyelocytic leukemia (APL): II. Clinical efficacy and pharmacokinetics in relapsed patients. Blood 1997;89:3354–60.

[5] Shao W, Fanelli M, Ferrara FF, Riccioni R, Rosenauer A, Davison K, Lamph WW, Waxman S, Pelicci PG, Lo Coco F, Avvisati G, Testa U, Peschle C, Gambacorti-Passerini C, Nervi C, Miller Jr. WH. Arsenic trioxide as an inducer of apoptosis and loss of PML/RARα protein in acute promyelocytic leukemia cells. J Natl Cancer Inst 1998;90:124–33.

[6] Wang ZG, Rivi R, Delva L, König A, Scheinbreg DA, Gambacorti-Passerini C, Gabrilove JL, Warrell RP, Pandolfi PP. Arsenic trioxide and melarsoprol induce programmed cell death in myeloïd leukemia cell lines and function in a PML and PML-RARα independent manner. Blood 1998;92:1497–504.

[7] Shen ZY, Shen J, Cai WJ, Hong C, Zheng MH. The alteration of mitochondria is an early event of arsenic trioxide induced apoptosis in esophageal carcinoma cells. Int J Mol Med 2000;5:155–8.

[8] Ora I, Bondesson L, Jönsson C, Ljungberg J, Pörn-Ares I, Garwicz S, Pahlman S. Arsenic trioxide inhibits neuroblastoma growth *in vivo* and promotes apoptotic cell death *in vitro*. Biochem Biophys Res Commun 2000;277:179–85.

[9] Huang SC, Huang CY, Lee TC. Induction of mitosis-mediated apoptosis by sodium arsenite in HeLa S3 cells. Biochem Pharmacol 2000;60:771–80.

[10] Uslu R, Sanli UA, Sezgin C, Karabulut B, Terzioglu E, Omay SB, Goker E. Arsenic trioxide-mediated cytotoxicity and apoptosis in prostate and ovarian carcinoma cell lines. Clin Cancer Res 2000;6:4957–64.

[11] Larochette N, Decaudin D, Jacotot E, Brenner C, Marzo I, Susin SA, Zamzami N, Xie Z, Reed JC, Kroemer G. Arsenite induces apoptosis via a direct effect on the mitochondrial permeability transition pore. Exp Cell Res 1999;249:413–21.

[12] Chen GQ, Zhu J, Shi XG, Ni JH, Zhong HJ, Si GY, Jin XL, Tang W, Li XS, Xong SM, Shen ZX, Sun GL, Ma J, Zhang P, Zhang TD, Gazin C, Naoe T, Chen SJ, Wang ZY, Chen Z. *In vitro* studies and cellular mechanisms of arsenic trioxide ($As_2O_3$) in the treatment of acute promyelocytic leukemia: $As_2O_3$ induces $NB_4$ cell apoptosis with downregulation of BCl-2 expression and modulation of PML-RARα/PML proteins. Blood 1996;88:1052–61.

[13] Hoffman RD, Lane MD. Iodophenylarsine oxide and arsenical affinity chromatography: new probes for dithiol proteins. Application to tubulins and to components of the insulin receptor-glucose transporter signal transduction pathway. J Biol Chem 1992;267:14005–11.

[14] Park WH, Seol JG, Kim ES, Hyun JM, Jung CW, Lee CC, Kim BK, Lee YY. Arsenic trioxide-mediated growth inhibition in MC/CAR myeloma cells via cell cycle arrest in association with induction of cyclin-dependent kinase inhibitor, p21, and apoptosis. Cancer Res 2000;60:3065–71.

[15] Ochi T. Induction of centrosome injury, multipolar spindles and multipolar division in cultured V79 cells exposed to dimethylarsinic acid: role for microtubules in centrosome dynamics. Mutat Res 2000;454:21–33.

[16] Eguchi N, Kuroda K, Endo G. Metabolites of arsenic induced tetraploids and mitotic arrest in cultured cells. Arch Environ Contam Toxicol 1997;32:141–5.

[17] Yager JW, Wiencke JK. Inhibition of poly(ADP ribose) polymerase by arsenite. Mutat Res 1997;386:345–51.

[18] Li YM, Broome JD. Arsenic targets tubulins to induce apoposis in myeloid leukemia cells. Cancer Res 1999;59:776–80.

[19] Chen F, Lu Y, Zhang Z, Vallyathan V, Ding M, Castranova V, Shi X. Opposite effect of NF-kappa B and c-Jun N-terminal kinase on p53-independent GADD45 induction by arsenite. J Biol Chem 2001;276:1414–9.

[20] Eisenhauer EA, Vermorken JB. The taxoids. Comparative clinical pharmacology and therapeutic potential. Drugs 1998;55:5–30.

[21] Doz F, Gentet JC, Frappaz D, Chastagner P, Moretti S, Vassal G, Arditti J, Tellingen O Van, Iliadis A, Catalin J. Phase I trial and pharmacological study of a 3-hr paclitaxel infusion in children with refractory solid tumours: a SFOP study. Br J Cancer 2001;84:604–10.

[22] Goncalves A, Braguer D, Kamath K, Martello L, Briand C, Horwitz S, Wilson L, Jordan MA. Resistance to Taxol in lung cancer cells associated with increased microtubule dynamics. PNAS 2001;98:11737–41.

[23] Wang LG, Liu XM, Kreis W, Budman DR. The effect of antimicrotubule agents on signal transduction pathways of apoptosis: a review. Cancer Chemother Pharmacol 1999;44:335–61.

[24] Bourgarel-Rey V, Vallee S, Rimet O, Champion S, Braguer D, Desobry A, Briand C, Barra Y. Involvement of nuclear factor κB in c-Myc induction by tubulin polymerization inhibitors. Mol Pharmacol 2001;59:1165–76.

[25] Goncalves A, Braguer D, Carles G, André N, Prévôt C, Briand C. Caspase-8 activation independent of CD95/CD95-L interaction during paclitaxel-induced apoptosis in human colon cancer cells (HT29-D4). Biochem Pharmacol 2000;60:1579–84.

[26] André N, Braguer D, Brasseur G, Goncalves A, Lemesle-Meunier D, Guise S, Jordan MA, Briand C. Paclitaxel induces release of cytochrome *c* from mitochondria isolated from human neuroblastoma cells. Cancer Res 2000;60:5349–53.
[27] Martello LA, McDaid HM, Regl DL, Yang CPH, Meng D, Pettus TRR, Kaufman MD, Arimoto H, Danishefsky SJ, Smith III AB, Horwitz SB. Taxol and discodermolide represent a synergistic drug combination in human carcinoma cell lines. Clin Cancer Res 2000;6:1978–87.
[28] Carles G, Braguer D, Sabeur G, Briand C. The effect of combining antitubulin agents on differentiated and undifferentiated human colon cancer cells. Anti-Cancer Drugs 1998;9:209–21.
[29] Fracasso PM, Brady MF, Moore DH, Walker JL, Rose PG, Letvak L, Grogan TM, McGuire WP. Phase II study of paclitaxel and valspodar (psc 833) in refractory ovarian carcinoma: a gynecologic oncology group study. J Clin Oncol 2001;19:2975–82.
[30] Nabholtz JM, Slamon D. New adjuvant strategies for breast cancer: meeting the challenge of integrating chemotherapy and trastuzumab (Herceptin). Semin Oncol 2001;28:1–12.
[31] Kohn EC, Reed E, Sarosy GA, Minasian L, Bauer KS, Bostick-Bruton F, Kulpa V, Fuse E, Tompkins A, Noone M, Goldspiel B, Pluda J, Figg WD, Liotta LAA. Phase I trial of carboxyamidotriazole and paclitaxel for relapsed solid tumors: potential efficacy of the combination and demonstration of pharmacokinetic interaction. Clin Cancer Res 2001;7:1600–9.
[32] Williams JI, Weitman S, Gonzalez CM, Jundt CH, Marty J, Stringer SD, Holroyd KJ, Mclane MP, Chen Q, Zasloff M, Von Hoff DD. Squalamine treatment of human tumors in nu/nu mice enhances platinum-based chemotherapies. Clin Cancer Res 2001;7:724–33.
[33] Sirotnak FM, Zakowski MF, Miller VA, Scher HI, Kris MG. Efficacy of cytotoxic agents against human tumor xenografts is markedly enhanced by coadministration of ZD1839 (Iressa), an inhibitor of EGFR tyrosine kinase. Clin Cancer Res 2000;6:4885–92.
[34] Hahm HA, Dunn VR, Butash KA, Deveraux WL, Woster PM, Casero Jr. RA. Davidson NE. Combination of standard cytotoxic agents with polyamine analogues in the treatment of breast cancer cell lines. Clin Cancer Res 2001;7:391–9.
[35] De Lena M, Lorusso V, Latorre A, Fanizza G, Gargano G, Caporusso L, Guida M, Catino A, Crucitta E, Sambiasi D, Mazzei A. Paclitaxel, cisplatin and lonidamine in advanced ovarian cancer. A phase II study. Eur J Cancer 2001;37:364–8.
[36] Gianni M, Koken MHM, Chelbi-Alix MK, Benoit G, Lanotte M, Chen Z, de Thé H. Combined arsenic and retinoic acid treatment enhances differenciation and apoptosis in arsenic-resistant NB4 cells. Blood 1998;91:4300–10.
[37] Jing Y, Wang L, Xia L, Chen GQ, Chen Z, Wilson HM, Waxman S. Combined effect of all-*trans*-retinoic acid and arsenic trioxide in acute promyelocytic leukemia cells *in vitro* and *in vivo*. Blood 2001; 97:264–9.
[38] Bachleitner-Hofmann T, Gisslinger B, Grumbeck E, Gisslinger H. Arsenic trioxide and ascorbic acid: synergy with potential implications for the treatment of acute myeloïd leukemia? Br J Haematol 2001;112:783–6.
[39] Kwong YL, Au WY, Chim CS, Pang A, Suen C, Liang R. Arsenic trioxide- and idarubicin-induced remissions in relapsed acute promyelocytic leukemia: clinicopathological and molecular features of a pilot study. Am J Hematol 2001;66:274–9.
[40] Guise S, Braguer D, Remacle-Bonnet M, Pommier G, Briand C. Tau protein is involved in the apoptotic process induced by anti-microtubule agents on neuroblastoma cells. Apoptosis 1999;4:47–58.
[41] Guise S, Braguer D, Carles G, Delacourte A, Briand C. Hyperphosphorylation of tau is mediated by ERK activation during anticancer drug-induced apoptosis in neuroblastoma cells. J Neurosci Res 2001; 63:257–67.
[42] Carles G, Braguer D, Dumontet C, Bourgarel V, Gonçalves A, Sarrazin M, Rognoni JB, Briand C. Differentiation of human colon cancer cells changes the expression of β-tubulin isotypes and MAPs. Br J Cancer 1999;80:1162–8.
[43] Chou TC, Talalay P. Quantitative analysis of dose–effect relationships: the combined effects of multiple drugs or enzyme inhibitors. Adv Enzyme Regul 1984;22:27–55.
[44] Garcia P, Braguer D, Carles G, Briand C. Simultaneous combination of microtubule depolymerizing and stabilizing agents acts at low doses. Anti-Cancer Drugs 1995;6:533–44.
[45] Weisenberg RC, Borisy GG, Taylor EW. The colchicine-binding protein of mammalian brain and its relation to microtubules. Biochemistry 1968;7:4466–79.
[46] Barbier P, Gregoire C, Devred F, Sarrazin M, Peyrot V. In vitro effect of Cryptophycin 52 on microtubule assembly and tubulin: molecular modeling of the mechanism of action of a new antimitotic drug. Biochemistry 2001;40:13510–9.
[47] Evangelio JA, Abal M, Barasoain I, Souto AA, Lillo MP, Acuna AU, Amat-Guerri F, Andreu JM. Fluorescent taxoids as probes of the microtubule cytoskeleton. Cell Motil Cytoskeleton 1998;39:73–90.
[48] Legault J, Gaulin JF, Mounetou E, Bolduc S, Lacroix J, Poyet P, Gaudreault RC. Microtubule disruption induced *in vivo* by alkylation of beta-tubulin by 1-aryl-3-(2-chloroethyl)ureas, a novel class of soft alkylating agents. Cancer Res 2000;60:985–92.
[49] Combeau C, Provost J, Lancelin F, Tournoux Y, Prod'homme F, Herman F, Lavelle F, Leboul J, Vuilhorgne M. RPR112378 and RPR115781: two representatives of a new family of microtubule assembly inhibitors. Mol Pharmacol 2000;57:553–63.
[50] Huang SC, Lee TC. Arsenite inhibits mitotic division and perturbs spindle dynamics in HeLa S3 cells. Carcinogenesis 1998;19:889–96.
[51] Akao Y, Nakagawa Y, Akiyama K. Arsenic trioxide induces apoptosis in neuroblastoma cell lines through the activation of caspase 3 *in vitro*. FEBS Lett 1999;455:59–62.
[52] Ramirez P, Eastmond DA, Laclette JP, Ostrosky-Wegman P. Disruption of microtubule assembly and spindle formation as a mechanism for the induction of aneuploïd cells by sodium arsenite and vanadium pentoxide. Mutat Res 1997;386:291–8.
[53] Costantini P, Chernyak BV, Petronilli V, Bernardi P. Modulation of the mitochondrial permeability transition pore by pyridine nucleotides and dithiol oxidation at two separate sites. J Biol Chem 1996;271:6746–51.
[54] Belzacq AS, El Hamel C, Vieira HL, Cohen I, Haouzi D, Metivier D, Marchetti P, Brenner C, Kroemer G. Adenine nucleotide translocator mediates the mitochondrial membrane permeabilization induced by lonidamine, arsenite and CD437. Oncogene 2001;20:7579–87.
[55] Rodi DJ, Janes RW, Sanganee HJ, Holton RA, Wallace BA, Makwski L. Screening of a library of phage-displayed peptides identifies human Bcl-2 as a taxol binding protein. J Mol Biol 1999;285:197–203.
[56] Tchounwou PB, Wilson BA, Ishaque AB, Schneider J. Atrazine potentiation of arsenic trioxide-induced cytotoxicity and gene expression in human liver carcinoma cells (HepG2). Mol Cell Biochem 2001;222:49–59.
[57] Jaattela M. Heat shock proteins as cellular lifeguards. Ann Med 1999;31:261–71. (Review).
[58] Ravagnan L, Gurbuxani S, Susin SA, Maisse C, Daugas E, Zamzami N, Mak T, Jaattela M, Penninger JM, Garrido C, Kroemer G. Heat-shock protein 70 antagonizes apoptosis-inducing factor. Nat Cell Biol 2001;3:839–43.
[59] Beere HM, Wolf BB, Cain K, Mosser DD, Mahboubi A, Kuwana T, Tailor P, Morimoto RI, Cohen GM, Green DR. Heat-shock protein 70 inhibits apoptosis by preventing recruitment of procaspase-9 to the Apaf-1 apoptosome. Nat Cell Biol 2000;2:469–75.